Research Article

INTERNATIONAL JOURNAL OF ADVANCED ROBOTIC SYSTEMS

International Journal of Advanced Robotic Systems
May-June 2019: 1–16

DOI: 10.1177/1729881419846712
journals.sagepub.com/home/arx
SAGE

Joint torque control of flexible joint robots based on sliding mode technique

Gen-Liang Xiong[1], Hai-Chu Chen[1], Jing-Xin Shi[2] and Fa-Yun Liang[1]

Abstract

For robots with flexible joints, the joint torque dynamics makes it difficult to control. An effective solution is to carry out a joint torque controller with fast enough dynamic response. This article is dedicated to design such a torque controller based on sliding mode technique. Three joint torque control approaches are proposed: (1) The proportional-derivative (PD)-type controller has some degree of robustness by properly selecting the control gains. (2) The direct sliding mode control approach which fully utilizes the physical properties of electric motors. (3) The sliding mode estimator approach was proposed to compensate the parameter uncertainties and the external disturbances of the joint torque system. These three joint torque controllers are tested and verified by the simulation studies with different reference torque trajectories and under different joint stiffness.

Keywords

Torque control, flexible joint, sliding mode

Date received: 22 February 2018; accepted: 2 April 2019

Topic: Robot Manipulation and Control
Topic Editor: Andrey V Savkin
Associate Editor: Alexander Pogromsky

Introduction

A robot manipulator with flexible joints[1–3] is normally not intended by the robot designer. Joint flexibility is a side effect when achieving a relative lightweight, for example, for space or medicine applications. Therefore, how to treat the joint torque dynamics makes the different control approaches for this kind of robots.

During the past decade, various methods have been proposed in order to control flexible joint robots. Theoretically, there is a general approach to control flexible joint robots (a large class of nonlinear systems) which is able to achieve fast response as well as "high bandwidth," namely the state-space approach based on the feedback linearization,[4,5] though some of nonlinear systems are not feedback linearizable. The disadvantage of this approach is the need for higher order time derivatives of the system output (i.e. the variable to be controlled). For the case of flexible joint robots, from the second time derivative of the link position one can only see the joint torque. And, from the fourth time derivative of the link position one can see the motor current. Only from the fifth time derivative of the link position one can see the final system control input, namely the stator voltage of the electric motor. Therefore, for the control design using the state-space approach, one needs up to the fourth time derivatives of the link position signal. As a result, the state-space approach based on the feedback

[1] School of Mechanical Engineering, Nanchang University, Nanchang, China
[2] School of Information Engineering, Nanchang University, Nanchang, China

Corresponding author:
Gen-Liang Xiong, School of Mechanical Engineering, Nanchang University, No. 999, XuFu Avenue, HongGuTan District, Nanchang, JiangXi Province, China.
Email: xionggenliang@ncu.edu.cn

linearization is not adequate for the control of flexible joint robots.

Another methodology to control flexible joint robots is to decompose the high-order system into two or more lower order subsystems. One of the control methods under this category is the cascaded control method.[6] It is well known that for classical cascaded control, the reference input to the inner control loop must be kept "constant" (means changing slowly) during the convergence of the inner control loop, implying that the response time of the total control system is slowed down due to the cascaded structure, resulting in a lower bandwidth with respect to the state-space approach. This is the price one has to pay for the advantages of the cascaded control method. The latter approach is the famous singular perturbation approach[7,8] as well as the integral manifold approach[9] which takes the joint torque subsystem as an algebraic system for the link position control and adds some damping to the fast mode in the joint torque.

In addition, other methods have also been proposed for flexible joint robot control, such as integral backstepping approach,[10] passivity-based control approach,[11] adaptive control technique,[12] fuzzy logic and neural network approaches,[13] and simple PD (or proportional-integral-derivative (PID)) control.[14] However, most of these control methods focus on position control and pay little attention to joint torque dynamics.

As mentioned in the study by Amjadi et al.,[15] singular perturbation approach is a smart solution to handle the joint torque dynamics. However, singular perturbation approach does not possess the tracking capability to follow a joint torque trajectory and it is only a solution based on some practice considerations. And now the question may arise: Why the tracking capability to follow a joint torque trajectory is required? Firstly, the composite control structure based on singular perturbation approach as well as integral manifold approach, viewed as a standard control structure for flexible joint robots, has the feature of open-loop control of joint torque dynamics, thus lack of robustness. This weakness has been observed by some researchers.[16] For example, if the joint stiffness changes, the controller based on singular perturbation approach does not possess the mechanisms to follow this change. Secondly, for a high-performance force or impedance control with a reasonable dynamic response in end-effector coordinate frame, the joint torque tracking capability is necessary. Imagining that an end-effector is grasping a moving workpiece, the control system must have a fast enough dynamic response, and the joint torque tracking controller will make this possible. Moreover, the dynamic motion of human arms is actually based on the joint torque feedback (thinking on an extreme case when a blind person touches his environment).

As a result, joint torque tracking capability is important for the control of a high-performance flexible joint robot. Though it is a difficult task to design a robust joint torque controller, joint torque control characterizes the main difference between the classic control and the modern control of flexible joint robots. Sliding mode control approach is the promising control approaches for the control of real-world high-order, nonlinear, multiple-input and multiple-output uncertain system, such as flexible joint robots and nonholonomic constrained mobile robots,[17–19] because they introduce proper physical information or utilize the physical property of controlled plant to make the solution simple and effective, rather than to play mathematical games. It is pointed out that modern sliding mode control theories have great potential to the control problems in this area. So, in this article, three different joint torque controllers based on sliding mode technique for multiple-link flexible joint robots will be proposed, verified, and compared by simulation studies.

Dynamic model

The model of a flexible joint robot manipulator with n degrees of freedom can be written as

$$\begin{cases} M(q)\ddot{q} + C(q,\dot{q})\dot{q} + G(q) + F(\dot{q}) = \tau \\ J\ddot{\theta} + \tau_{ds} + \tau = \boldsymbol{\Gamma}\tau_m \\ \tau = K(\theta - q) \end{cases} \tag{1}$$

where $M(q) \in \Re^{n\times n}$ is the mass matrix, $C(q,\dot{q})\dot{q} \in \Re^n$ the vector including centrifugal and Coriolis forces, $G(q) \in \Re^n$ the gravity force vector, $F(\dot{q}) \in \Re^n$ the the friction force vector, $q \in \Re^n$ the link position vector, $\theta \in \Re^n$ the joint position vector, $\tau \in \Re^n$ the joint torque vector, $\tau_m \in \Re^n$ the motor torque vector, $\tau_{ds} \in \Re^n$: disturbance torque vector, $J = [J_i] \in \Re^{n\times n}$ the diagonal joint inertia matrix, $K = [k_i] \in \Re^{n\times n}$ the diagonal joint stiffness matrix, and $\boldsymbol{\Gamma} = [\gamma_i] \in \Re^{n\times n}$ the diagonal gear ratio matrix.

Taking joint torque τ and link position q as state variables, model (1) can be reformulated as

$$\begin{cases} M(q)\ddot{q} + C(q,\dot{q})\dot{q} + G(q) + F(\dot{q}) = \tau \\ JK^{-1}\ddot{\tau} + \tau_{ds} + \tau + J\ddot{q} = \boldsymbol{\Gamma}\tau_m \end{cases} \tag{2}$$

The second equation of equation (2) represents the joint torque dynamics. Note that from the first equation of equation (2) we know $\partial\ddot{q}/\partial\tau_m = 0$, implying that term $J\ddot{q}$ can be treated as disturbance when designing joint torque controller based on the second equation of equation (2) using control input $\boldsymbol{\Gamma}\tau_m$. For the ith joint, the joint torque dynamics can be obtained by simply writing the second equation of equation (2) in component-wise

$$J_i K_i^{-1}\ddot{\tau}_i + \tau_{dsi} + \tau_i + J_i\ddot{q}_i = \gamma_i\tau_{mi} \tag{3}$$

It seems that the above equation about the joint torque is decoupled; this is because that the coupling effects from the other joints are acted through the joint acceleration $\ddot{q}_i$ which is not yet replaced by the first equation (i.e. the robot arm equation) of equation (2).

In order to see the dynamic behavior of the joint torque more clearly, $\ddot{q}$ in the second equation of equation (2) can

be replaced by solving $\ddot{q}$ from the first equation, resulting in the new formulation of the joint torque dynamics

$$\ddot{\tau} + A_\tau(t)\tau + D(t) = B_\tau \tau_m \tag{4}$$

where

$$A_\tau(t) = K\left(J^{-1} + M(q)^{-1}\right)$$

$$D_\tau(t) = K\left(J^{-1}\tau_{ds} + M(q)^{-1}N(q,\dot{q})\right)$$

$$B_\tau = KJ\Gamma$$

$$N(q,\dot{q}) = C(q,\dot{q})\dot{q} + G(q) + F(\dot{q})$$

Since matrix $M(q)^{-1}$ is not a diagonal matrix, we can see the coupling effects:

(a) The disturbance vector $D_\tau(t)$ contains all time-varying parameters of robot arm through term $M(q)^{-1}N(q,\dot{q})$.
(b) The joint torque dynamics of one joint are influenced by the joint torques of all other joints through matrix $A_\tau(t)$, implying that the joint torques are interconnected between the joints.

Taking a two-link flexible joint robot as an example, the joint torque dynamics for the two joints can be derived as

$$\begin{cases} \ddot{\tau}_1 + k_1(J_1^{-1} + zm_{22})\tau_1 - k_1 zm_{12}\tau_2 + [k_1 J_1^{-1} f_1 + k_1(zm_{22}n_1 - zm_{12}n_2)] = k_1 J_1^{-1}\gamma_1\tau_{m1} \\ \ddot{\tau}_2 + k_2(J_2^{-1} + zm_{11})\tau_2 - k_2 zm_{21}\tau_1 + [k_2 J_2^{-1} f_2 + k_2(zm_{11}n_2 - zm_{21}n_1)] = k_2 J_2^{-1}\gamma_2\tau_{m2} \end{cases} \tag{5}$$

where $z = 1/(m_{11}m_{22} - m_{12}m_{21})$. Note that parameters m_{ij} and n_i (with $i = 1, 2$ and $j = 1, 2$) are time-varying.

For the decentralized joint torque control design, it is preferred to use model (3), because of the simplicity. Since parameter uncertainties and unknown disturbances exist, robust control approaches are necessary.

Joint torque control by PD controller

For the analysis of the PD type of joint torque controller for the ith joint, model (3) is cleaned by removing subscript i (keep in mind that we now deal with the torque control of one joint, i.e. the decentralized joint torque control problem)

$$JK^{-1}\ddot{\tau} + \tau_{ds} + \tau + J\ddot{q} = \gamma\tau_m \tag{6}$$

We know that motor torque τ_m is generated by the motor stator current i_q with the relation $\tau_m = k_t i_q$, with k_t being the torque constant of the permanent magnet synchronous motor (PMSM) used for the joint. So that the actual control input of the torque dynamics is the motor stator current i_q, that is

$$\frac{J}{k\gamma k_t}\ddot{\tau} + \frac{1}{\gamma k_t}(\tau_{ds} + \tau) + \frac{J}{\gamma k_t}\ddot{q} = i_q \tag{7}$$

Now the control task is: Look for the reference current i_q^* which enables the tracking of the actual joint torque τ to the reference joint torque τ_d. The resulting i_q^* will be fitted to the inner current control loop as the reference input. For the PD-type joint torque controller (see Appendix 1, Fig.A1) for system (7), i_q^* can be designed as

$$i_q^* = \begin{cases} i_{q\_\max} & \text{if}(-k_d\dot{e}_\tau - k_p e_\tau) \geq i_{q\_\max} \\ -k_d\dot{e}_\tau - k_p e_\tau & \text{if}|k_d\dot{e}_\tau + k_p e_\tau| < i_{q\_\max} \\ -i_{q\_\max} & \text{if}(-k_d\dot{e}_\tau - k_p e_\tau) \leq -i_{q\_\max} \end{cases} \tag{8}$$

where $e_\tau = \tau_d - \tau$ is the torque control error and i_q^* is limited to $\pm i_{q\_\max}$. Because $\ddot{q}$ is normally not measured, it has to be treated as a disturbance term. Also some parameters like J, k, k_t and disturbance torque τ_{ds} are generally unknown. Therefore, we expect the PD controller should provide some degree of robustness to these uncertainties. Now, it will be shown that by properly adjusting the control gains k_p and k_d, in order to avoid the chattering effect of PD controller. Therefore, the PD controller will have some degree of robustness by properly selecting the control gains.

However, since the resulting reference current i_q^* is discontinuous, it would cause problem for the inner current control loop, especially for the case where the standard PWM technique for the current control is used. The duty-cycle feeding to the pulse width modulation (PWM) unit would jump suddenly from one value to another which is harmful to the actuator and introduces high-frequency vibration. Therefore, a continuous saturation function is employed instead of the discontinuous current i_q^* to smooth the reference current.

For the inner current control loop, either the conventional PWM technique or PD current control can be used. For the simulation studies given in this article the latter is used. Note that for the joint torque control we need only to control the stator current component i_q, but current component i_d has influence to the control of i_q. For the joint torque control purpose, we will set the reference current $i_d^* = 0$, with which the dynamics of current component i_q will be decoupled from the ones of i_d and the motor is able to work in the so-called constant torque mode.

Joint torque control by direct sliding mode control

In the previous section, we discussed the cascaded control structure for the joint torque control, with inner current

control loop and outer PD-type joint torque control loop. This control structure has some advantages, namely:

(a) the designs of the joint torque control and the current control can be done separately;
(b) it is easier for the implementation and for the tuning of the controller parameters; and
(c) only first time derivative of the joint torque signal is required.

However, there are some disadvantages with this simple control system:

(a) The cascaded control structure limits the bandwidth of the closed-loop system.
(b) The system robustness is limited.
(c) The torque control system will not work properly if the joint torque dynamics are faster than the ones of motor current, this will happen when the joint stiffness is high, that is, the robot is more rigid.
(d) Large chattering may occur if the control gains of the PD controller are too high.

In the following, we propose a direct (non-cascaded) joint torque control schema without using the conventional PWM, which is dedicated to overcome these disadvantages. The proposed new control schema has the following features:

(a) It fully utilizes the property of electric motors, namely, the final control signals of the power converter (i.e. inverter) have to be discontinuous, no matter which control strategy is employed and no matter which state variables of the robot are controlled.
(b) The inner current control loop for the q-component is removed. This motor current component is then implicitly controlled through the control of the second time derivative of the joint torque, resulting in a state-space control schema, thus increasing the system bandwidth.
(c) The stability of the closed-loop torque tracking control system can be proved and the robustness with respect to the system uncertainties can be guaranteed.

As control design tool, we use again the sliding mode control theory. The system model used for the decentralized joint torque control for ith joint (subscript i is removed for simplicity) is given as

$$\begin{cases} \dfrac{J}{k\gamma k_t}\ddot{\tau} + \dfrac{1}{\gamma k_t}(\tau + \tau_{ds}) + \dfrac{J}{\gamma k_t}\ddot{q} = i_q \\ L\dfrac{\mathrm{d}i_d}{\mathrm{d}t} = u_d - Ri_d + L\omega_e i_q \\ L\dfrac{\mathrm{d}i_q}{\mathrm{d}t} = u_q - Ri_q - L\omega_e i_d - \lambda_0\omega_e \end{cases} \tag{9}$$

where ω_e is the rotor electrical angular speed, and the relation with the joint angular speed $\dot{\theta}$ is

$$\omega_e = P\dot{\theta}_m = P\gamma\dot{\theta} \tag{10}$$

with P being the number of pole pair of the PMSM and $\dot{\theta}_m$ being the rotor mechanical angular speed of PMSM. With the relation (10) and changing the order of the equations for i_d and i_q, we get the model to start the joint torque control design

$$\begin{cases} \dfrac{J}{k\gamma k_t}\ddot{\tau} + \dfrac{1}{\gamma k_t}(\tau + \tau_{ds}) + \dfrac{J}{\gamma k_t}\ddot{q} = i_q \\ L\dfrac{\mathrm{d}i_q}{\mathrm{d}t} = u_q - Ri_q - LP\gamma\dot{\theta}i_d - \lambda_0 P\gamma\dot{\theta} \\ L\dfrac{\mathrm{d}i_d}{\mathrm{d}t} = u_d - Ri_d + LP\gamma\dot{\theta}i_q \end{cases} \tag{11}$$

Taking the time derivative of the first equation in equation (11) and substituting with the second equation result in the third-order model for the joint torque related to the stator voltage u_q

$$\frac{JL}{k\gamma k_t}\dddot{\tau} + \frac{L}{\gamma k_t}(\ddot{\tau} + \ddot{\tau}_{ds}) + \frac{JL}{\gamma k_t}\dddot{q} = u_q - Ri_q - LP\gamma\dot{\theta}i_d - \lambda_0 P\gamma\dot{\theta} \tag{12}$$

Then, the system model (dynamics about the joint torque τ and about the stator current component i_d) can be given as

$$\begin{cases} \dddot{\tau} = -A^{-1}(B\ddot{\tau} + B\ddot{\tau}_{ds} + C\dddot{q} + E\ddot{\theta} + R\dot{i}_q + D\dot{\theta}\dot{i}_d) + A^{-1}\dot{u}_q \\ A^{-1}L\ddot{i}_d = -A^{-1}R\dot{i}_d + A^{-1}D\dot{\theta}\dot{i}_q + A^{-1}\dot{u}_d \end{cases} \tag{13}$$

where the following auxiliary parameters are introduced in order to simplify the notation

$$A = \frac{JL}{k\gamma k_t}, \quad B = \frac{L}{\gamma k_t}, \quad C = \frac{JL}{\gamma k_t}, \quad D = LP\gamma, \quad E = \lambda_0 P\gamma \tag{14}$$

Note that in the second equation of equation (13), both sides are multiplied with A^{-1}, such that both stator voltages u_d and u_q in equation (13) have the same coefficient, this will simplify the controller design.

Controller design

At first, the switching functions for the joint torque and for the d-component of the state current are designed see Appendix 1, Fig.A2

$$\begin{cases} s_\tau = \ddot{e}_\tau + c_1\dot{e}_\tau + c_0 e_\tau \\ s_d = A^{-1}L(i_d - i_d^*) \end{cases} \tag{15}$$

where $e_\tau = \tau_d - \tau$ is the joint torque control error. Note that the parameter $A^{-1}L$ is introduced in s_d to simplify the control design. The controller will depend on this parameter any way, when not multiplied here, it must be involved in the sliding mode transformation given later.

The time derivative of both switching functions along the solutions of equation (13) can be derived as

$$\begin{cases} \dot{s}_\tau = -\dddot{\tau}_d + c_1\ddot{e}_\tau + c_0\dot{e}_\tau - A^{-1}(B\ddot{\tau} + B\ddot{\tau}_{ds} + C\dddot{q} + E\ddot{\theta} + R\dot{i}_q + D\ddot{\theta}i_d) + A^{-1}u_q \\ \dot{s}_d = -A^{-1}L\dot{i}_d^* - A^{-1}Ri_d + A^{-1}D\dot{\theta}i_q + A^{-1}u_d \end{cases} \tag{16}$$

Introducing two auxiliary variables f_τ and f_d as follows

$$\begin{cases} f_\tau = -\dddot{\tau}_d + c_1\ddot{e}_\tau + c_0\dot{e}_\tau - A^{-1}(B\ddot{\tau} + B\ddot{\tau}_{ds} + C\dddot{q} + E\ddot{\theta} + R\dot{i}_q + D\ddot{\theta}i_d) \\ f_d = -A^{-1}L\dot{i}_d^* - A^{-1}Ri_d + A^{-1}D\dot{\theta}i_q \end{cases} \tag{17}$$

Equation (16) will be simplified to

$$\begin{cases} \dot{s}_\tau = f_\tau + A^{-1}u_q \\ \dot{s}_d = f_d + A^{-1}u_d \end{cases} \tag{18}$$

Note that for these two auxiliary variables, $\partial f_\tau/\partial u_q = 0$ and $\partial f_d/\partial u_d = 0$ hold, this is necessary for the sliding mode control design. The above equation system can be summarized in the vector form (the sequence of the both equations is exchanged to match the sequence of u_d and u_q in the context of electric motors), resulting in

$$\begin{bmatrix} \dot{s}_d \\ \dot{s}_\tau \end{bmatrix} = \begin{bmatrix} f_d \\ f_\tau \end{bmatrix} + A^{-1}\begin{bmatrix} u_d \\ u_q \end{bmatrix} \tag{19}$$

From the study by Ademi and Jovanović,[20] we know that the stator voltages u_d and u_q are not yet the discontinuous voltages applied to the motor windings. For the direct sliding mode control design, we need the relation between the final discontinuous voltages applied to the motor windings and the time derivative of both switching functions. This relation can be found by using the definition given in

$$\begin{bmatrix} \dot{s}_d \\ \dot{s}_\tau \end{bmatrix} = \begin{bmatrix} f_d \\ f_\tau \end{bmatrix} + A^{-1}\begin{bmatrix} u_d \\ u_q \end{bmatrix} = \begin{bmatrix} f_d \\ f_\tau \end{bmatrix} + A^{-1}A_{d,q}^{1,2,3}\begin{bmatrix} u_1 \\ u_2 \\ u_3 \end{bmatrix} \tag{20}$$

where matrix $A_{d,q}^{1,2,3}$ can be expanded as

$$A_{d,q}^{1,2,3} = A_{d,q}^{a,b,c} = A_{d,q}^{\alpha,\beta}A_{\alpha,\beta}^{a,b,c} = \begin{bmatrix} \cos\theta_a & \cos\theta_b & \cos\theta_c \\ -\sin\theta_a & -\sin\theta_b & -\sin\theta_c \end{bmatrix} \tag{21}$$

With $\theta_a = \theta_e$, $\theta_b = \theta_e - 2\pi/3$, $\theta_c = \theta_e + 2\pi/3$ and θ_e being the rotor electrical angular position. Depending on equation (21), equation (20) can be rewritten as

$$\begin{bmatrix} \dot{s}_d \\ \dot{s}_\tau \end{bmatrix} = \begin{bmatrix} f_d \\ f_\tau \end{bmatrix} + A^{-1}\begin{bmatrix} u_1\cos\theta_a + u_2\cos\theta_b + u_3\cos\theta_c \\ -u_1\sin\theta_a - u_2\sin\theta_b - u_3\sin\theta_c \end{bmatrix} \tag{22}$$

To find the control signals u_1, u_2, and u_3, Lyapunov approach will be employed. Design a Lyapunov function candidate as

$$V = \frac{1}{2}\boldsymbol{s}_{d\tau}^{\mathrm{T}}\boldsymbol{s}_{d\tau} \tag{23}$$

where $\boldsymbol{s}_{d\tau} = [s_d\ s_\tau]^{\mathrm{T}}$. The time derivative of V along the solution of equation (22) can be found as (note that parameter A is a scalar value and not a matrix, see the definition in equation (14))

$$\begin{aligned} \dot{V} &= \boldsymbol{s}_{d\tau}^{\mathrm{T}}\dot{\mathbf{s}}_{d\tau} = [s_d\ \ s_\tau]\begin{bmatrix} \dot{s}_d \\ \dot{s}_\tau \end{bmatrix} \\ &= [s_d\ \ s_\tau]\begin{bmatrix} f_d \\ f_\tau \end{bmatrix} + A^{-1}[s_d\ \ s_\tau]\begin{bmatrix} u_1\cos\theta_a + u_2\cos\theta_b + u_3\cos\theta_c \\ -u_1\sin\theta_a - u_2\sin\theta_b - u_3\sin\theta_c \end{bmatrix} \end{aligned} \tag{24}$$

Equation (24) can be further expanded as

$$\begin{aligned} \dot{V} &= \boldsymbol{s}_{d\tau}^{\mathrm{T}}\dot{\mathbf{s}}_{d\tau} \\ &= (s_d f_d + s_\tau f_\tau) \\ &\quad + A^{-1}(u_1 s_d\cos\theta_a + u_2 s_d\cos\theta_b + u_3 s_d\cos\theta_c - u_1 s_\tau\sin\theta_a - u_2 s_\tau\sin\theta_b - u_3 s_\tau\sin\theta_c) \\ &= (s_d f_d + s_\tau f_\tau) \\ &\quad + A^{-1}[u_1(s_d\cos\theta_a - s_\tau\sin\theta_a) + u_2(s_d\cos\theta_b - s_\tau\sin\theta_b) + u_3(s_d\cos\theta_c - s_\tau\sin\theta_c)] \end{aligned} \tag{25}$$

Introducing three additional auxiliary variables

$$\begin{cases} \Omega_1 = s_d\cos\theta_a - s_\tau\sin\theta_a \\ \Omega_2 = s_d\cos\theta_b - s_\tau\sin\theta_b \\ \Omega_3 = s_d\cos\theta_c - s_\tau\sin\theta_c \end{cases} \tag{26}$$

Equation (25) can be simplified to

$$\dot{V} = (s_d f_d + s_\tau f_\tau) + A^{-1}(u_1\Omega_1 + u_2\Omega_2 + u_3\Omega_3) \tag{27}$$

Equation (26) can be interpreted as a kind of sliding mode transformation which performs actually the

decoupling task for multi-inputs control systems, see also Utkin et al.[21] for more details. If $s_d = 0$ and $s_\tau = 0$, that is, sliding mode occurs, then $\Omega_i = 0$ ($i = 1, 2, 3$) as well.

In order to guarantee $\dot{V} < 0$, the control signals (i.e. the final discontinuous control voltages applied to the motor windings through the inverter) u_1, u_2, and u_3 can be designed as

$$\begin{cases} u_1 = -u_0 \text{sign}(\Omega_1) \\ u_2 = -u_0 \text{sign}(\Omega_2) \\ u_3 = -u_0 \text{sign}(\Omega_3) \end{cases} \tag{28}$$

where u_0 is the DC-bus voltage of the inverter. With these control signals, equation (27) can be reformulated for the final analysis

$$\begin{aligned} \dot{V} &= (s_d f_d + s_\tau f_\tau) - A^{-1} u_0 [\text{sign}(\Omega_1)\Omega_1 + \text{sign}(\Omega_2)\Omega_2 \\ &\quad + \text{sign}(\Omega_3)\Omega_3] \\ &= (s_d f_d + s_\tau f_\tau) - A^{-1} u_0 [|\Omega_1| + |\Omega_2| + |\Omega_3|] \end{aligned} \tag{29}$$

In the above equation, A^{-1} is a positive constant (but may not be known). If the scalar term $(s_d f_d + s_\tau f_\tau)$ is bounded and if the DC-bus voltage u_0 is high enough, $\dot{V} < 0$ can be guaranteed. Thus, the stability of the control system can be ensured under two conditions:

(a) the DC-bus voltage u_0 should be high enough, and
(b) auxiliary variables f_τ and f_d are bounded.

Since f_τ and f_d do not contain the control voltages, neither u_d and u_q nor u_1, u_2, and u_3, the condition (b) is reasonable. Actually, only term $C\ddot{q}$ in f_τ is doubtful. For this, we can write $\dddot{q} = \text{d}(\ddot{q})/\text{d}t$ in which $\ddot{q}$ can be replaced by the corresponding solution (means the solution in component-wise) after solving the first equation of equation (1) for $\ddot{q}$. This is to say, $\dddot{q}$ has no algebraic relation with u_q and condition (b) can be assumed. It will be shown in the later simulation studies that this assumption makes no problem for achieving desired control performance. It is a natural result of high-gain robust control theories including sliding mode control.

Implementation steps

Though the derivation of the proposed control system looks rather sophisticated, the implementation of the controller is quite simple.

Step 1: Calculating the joint torque error and the switching functions

$$\begin{cases} e_\tau = \tau_d - \tau \\ s_\tau = \ddot{e}_\tau + c_1 \dot{e}_\tau + c_0 e_\tau \\ s_d = A^{-1} L (i_d - i_d^*) \end{cases} \tag{30}$$

Step 2: Calculating the sliding mode transformation

$$\begin{cases} \Omega_1 = s_d \cos\theta_a - s_\tau \sin\theta_a \\ \Omega_2 = s_d \cos\theta_b - s_\tau \sin\theta_b \\ \Omega_3 = s_d \cos\theta_c - s_\tau \sin\theta_c \end{cases} \tag{31}$$

with $\theta_a = \theta_e$, $\theta_b = \theta_e - 2\pi/3$, $\theta_c = \theta_e + 2\pi/3$.
Step 3: Calculating the discontinuous control voltages

$$\begin{cases} u_1 = -u_0 \text{sign}(\Omega_1) \\ u_2 = -u_0 \text{sign}(\Omega_2) \\ u_3 = -u_0 \text{sign}(\Omega_3) \end{cases} \tag{32}$$

In equation (30), parameters c_0 and c_1 have to be provided by the control designer depending on the required closed-loop performance of the joint torque control. Parameter $A^{-1}L = k\gamma k_t/J$ is not easy to obtain and thus can be tuned, until $i_d = i_d^*$, then this parameter has no effect to the control system anymore. The real-world implementation of this direct sliding mode joint torque controller needs to change the popular hardware, because it bypasses the PWM unit within a microcontroller or a digital signal processor (DSP), but needs high enough sample time to handle the high-frequency phase signals (phase currents and phase voltages).

Joint torque control by SME

The dynamic model about the joint torques, that is, equation (4) (which is in matrix–vector form) can be rewritten in component-wise for the ith robot joint (here again, subscript i is not used for simplicity)

$$\ddot{\tau} + a(t)\tau + d(t) = b\tau_m \tag{33}$$

As discussed in the "Dynamic model" section, $a(t)$ is a function of the components of the robot mass matrix $M(q)$, and $d(t)$ is a function of the components of all dynamic terms in the first equation of equation (1) and a function of the joint torques of all other joints, see also equation (5) as an example. We assume that parameters $a(t)$, $d(t)$, and b in equation (33) are unknown, but bounded. For the implementation of the control algorithm, we need a rough estimate (or called nominal value) of $a(t)$ and b, denoted as $\hat{a}$ and $\hat{b}$, respectively. Then, the joint torque controller based on the SME see Appendix 1, Fig.A3 can be applied to system (33) directly and summarized as follows

$$\begin{cases} \tau_f = \hat{b}^{-1}(\hat{a}\tau + \ddot{\tau}_d - c_1\dot{e}_\tau - c_0 e_\tau) \\ \hat{z}(0) = \dot{\tau}(0) \\ u_{eq} = \text{low-pass}\left(M_s \text{sign}(\hat{z} - \dot{\tau})\right) \\ \tau_r = \hat{b}^{-1} u_{eq} \\ \dot{\hat{z}} = \ddot{\tau}_d - c_1\dot{e}_\tau - c_0 e_\tau + \hat{b}\tau_r - M_s \text{sign}(\hat{z} - \dot{\tau}) \\ \tau_m = \tau_f + \tau_r \end{cases} \tag{34}$$

where $\hat{z}$ is the artificially introduced auxiliary variable, which is actually an estimate of $\dot{\tau}$. Parameters $\hat{a}$, $\hat{b}$, c_0, c_1, M_s, and the time constant of the low-pass filter have to be provided by the control designer. Disturbance term $d(t)$ in equation (33) is highly time-varying but unknown, thus it is not required by the controller implementation. The proof of stability see Appendix 1.

This joint torque controller needs an inner current control loop. Same as the "Joint torque control by PD controller" section, we will use the direct sliding mode current controller in the current control loop for the simulation study. The reference q-axis current feeding to the current controller is calculated by $i_q^* = \tau_m / k_t$, with k_t being the torque constant of the PMSM used in the robot joint. The reference d-axis current is set to $i_d^* = 0$ for the joint torque control task (sure, i_d^* can also be set to other values to achieve corresponding control performance).

Simulation studies

Plant model used for the simulation

To verify the proposed control approaches, we use a two-link flexible joint robot as the plant model, which consists of the two-link rigid-body robot model can be given as

$$\begin{bmatrix} m_{11} & m_{12} \\ m_{21} & m_{22} \end{bmatrix} \begin{bmatrix} \ddot{q}_1 \\ \ddot{q}_2 \end{bmatrix} + \begin{bmatrix} c_1 + g_1 + f_1 \\ c_2 + g_2 + f_2 \end{bmatrix} = \begin{bmatrix} \tau_1 \\ \tau_2 \end{bmatrix}, \text{ that is}$$
$$M(q) = \begin{bmatrix} m_{11} & m_{12} \\ m_{21} & m_{22} \end{bmatrix}, \quad N(q, \dot{q}) = \begin{bmatrix} c_1 + g_1 + f_1 \\ c_2 + g_2 + f_2 \end{bmatrix} \tag{35}$$

with

$$\begin{aligned} m_{22} &= L_2^2 M_2 \\ m_{12} &= m_{21} = m_{22} + L_1 L_2 M_2 \cos q_2 \\ m_{11} &= L_1^2 (M_1 + M_2) + 2m_{12} - m_{22} \\ c_1 &= -L_1 L_2 M_2 (2\dot{q}_1 \dot{q}_2 - \dot{q}_2^2) \sin q_2 \\ c_2 &= L_1 L_2 M_2 \dot{q}_1^2 \sin q_2 \\ g_2 &= L_2 M_2 g \cos(q_1 + q_2) \\ g_1 &= L_1 (M_1 + M_2) g \cos(q_1) + g_2 \\ f_1 &= k_{v1} \dot{q}_1 + k_{c1} \text{sign}(\dot{q}_1) \\ f_2 &= k_{v2} \dot{q}_2 + k_{c2} \text{sign}(\dot{q}_2) \end{aligned} \tag{36}$$

where k_{vi} and k_{ci} ($i = 1, 2$) are coefficients of viscous friction and coulomb friction, respectively.

The joint model given by the second and third equations of equation (1), the PMSM model in the AC-form and the voltage transformation were given by Ademi and Jovanović.[20] The final control inputs are the discontinuous control voltages applied to the three stator windings, that is u_1, u_2, and u_3, taking values from the discrete set $\{-u_0, +u_0\}$.

The parameters of the two-link flexible joint robot used for the simulation are listed in Tables 1 to 3. Note that for the simulation, the joint disturbance torque in equation (1) is selected as $\tau_{ds} = k_\omega \dot{\theta}$ for both joints.

Table 1. Arm parameters.

M_1 (kg)	M_2 (kg)	L_1 (m)	L_2 (m)
4	2	0.5	0.5

Table 2. Parameters for motor 1 and motor 2.

$L(H)$	R (Ω)	λ_0	P	k_t (Nm/A)	I_{q_max} (A)	U_0 (V)
44.5×10^3	0.68	0.24	4	$(3/2)P\lambda_0$	60	120

Table 3. Parameters of joint 1 and joint 2.

J (kg m^2)	k (Nm/rad)	γ	k_ω (Nm/(rad/s))
1.5	10,000	40	1

Reference inputs for testing the joint torque controllers

Three types of torque reference are fed to each of the three joint torque controllers:

(a) step input of 10 Nm with the step time at $t = 0$,
(b) 4 Hz sinusoidal input with 10 Nm amplitude for the case of small signal tracking, and
(c) 4 Hz sinusoidal input with 100 Nm amplitude for the case of large signal tracking.

To test the robustness of the joint torque controllers, the joint stiffness of both robot joints in the plant model is changed from 10,000 Nm/Rad to 1000Nm/Rad and the reference signals for the simulation are repeated from point (a) to point (c), in order to verify the behavior of the joint torque controllers in the case of very large joint compliance without changing the controller parameters.

Controller parameters

The parameters for the all three joint torque controllers are tuned to have a satisfactory torque control response for the case of step reference torque input of 10 Nm (i.e. point (a)). And then, these parameters remain unchanged for the all other simulation tests.

For the joint torque controller given in the "Joint torque control by PD controller" section, that is, the PD controller, only three parameters for each joint are required, k_p, k_d, and i_{q_max}. They are selected as

$$\begin{cases} k_{p1} = 4, & k_{d1} = 0.05, & i_{q1\_max} = 60A \\ k_{p2} = 4, & k_{d2} = 0.05, & i_{q2\_max} = 60A \end{cases} \tag{37}$$

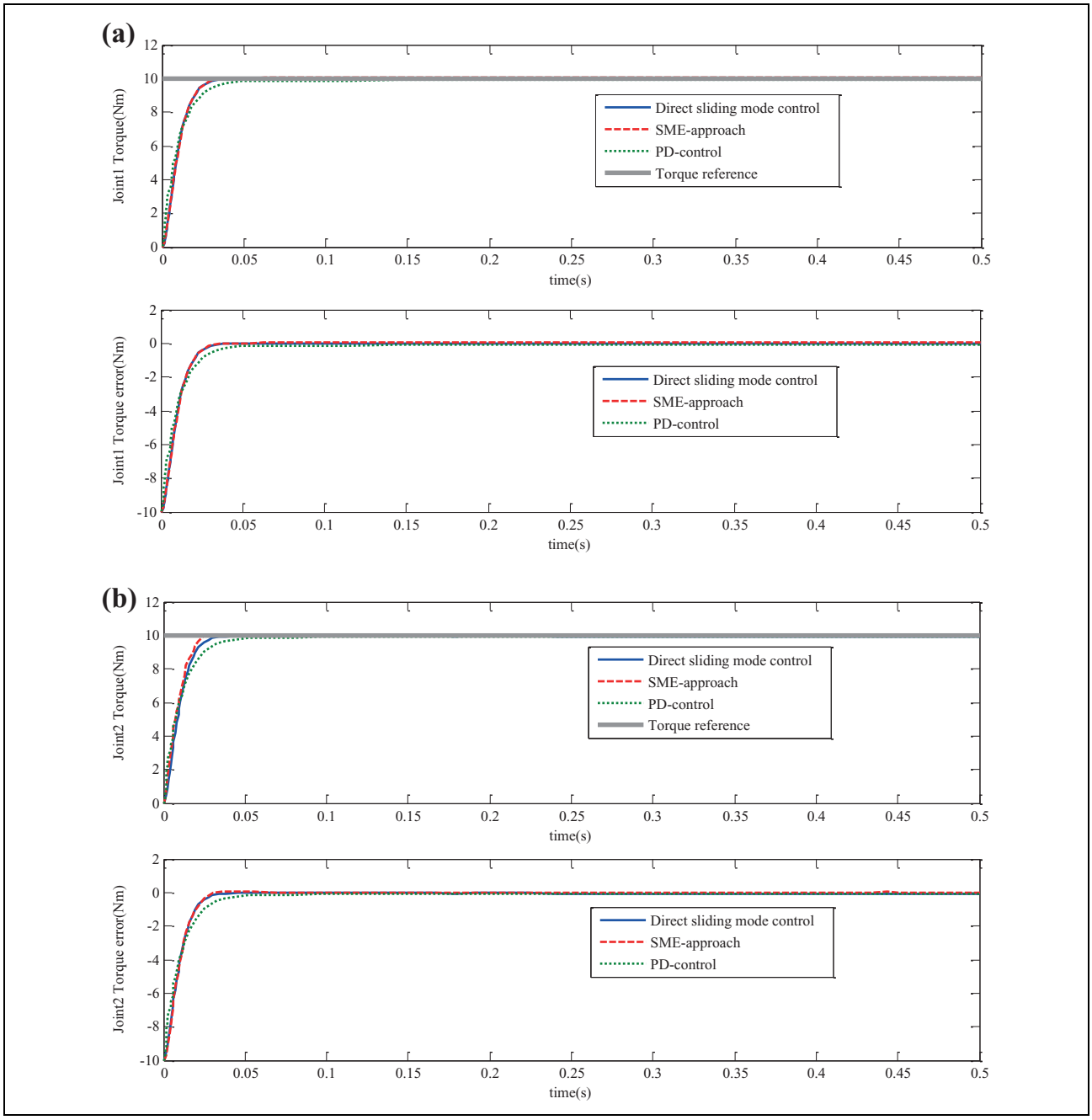

Figure 1. Step response of joint torque control: (a) response of joint 1 and (b) joint 2.

For the joint torque controller given in the "Joint torque control by direct sliding mode control" section, that is, the direct sliding mode control approach, we also need three parameters for each joint, c_0, c_1, and $A^{-1}L = k\gamma k_t/J$, see equation (30). Actually, parameter $A^{-1}L$ is dedicated for the construction of the sliding surface for the control of stator current i_d component (while stator current i_q component is not explicitly controlled). Simulation shows that the joint torque control system is not sensitive to this parameter, this result coincides with the theoretical expectation by the author. For the simulation, the controller parameters are selected as

$$\begin{cases} c_{01} = 20,000, & c_{11} = 200, & (A^{-1}L)_1 = 3.84 \times 10^5 \\ c_{02} = 20,000, & c_{12} = 200, & (A^{-1}L)_2 = 3.84 \times 10^5 \end{cases} \tag{38}$$

For the control approach given in the "Joint torque control by SME" section, that is, the SME approach, some nominal parameters are required for the pole placement

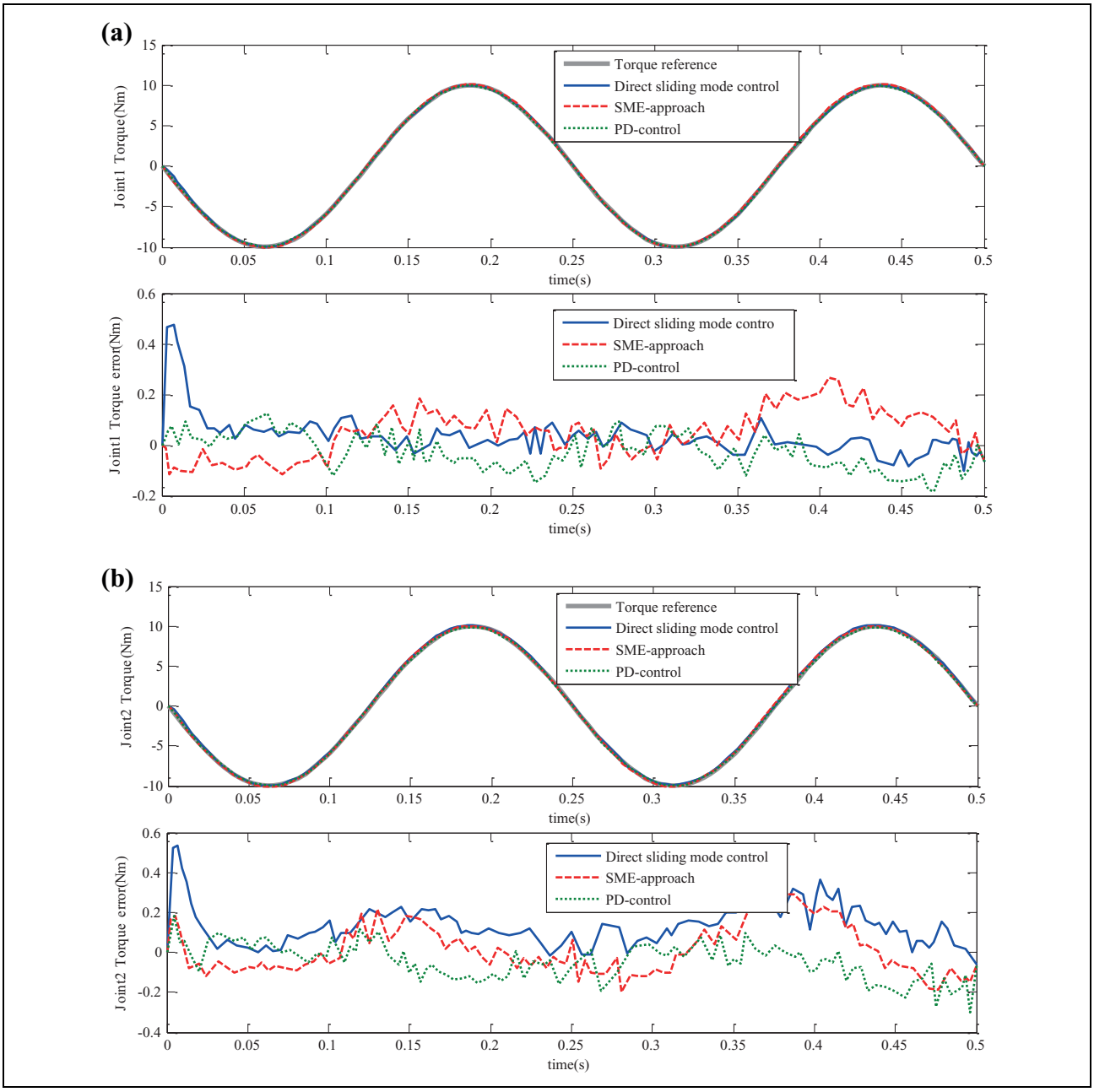

Figure 2. Sinusoidal torque reference (small amplitude): (a) response of joint 1 and (b) joint 2.

of the torque tracking control. These parameters are selected artificially to have some derivation with respect to their true counterparts (because their true values are actually unknown in practice).

$$\begin{cases} J_{m1\_n} = 1.3J_1/\gamma_1^2 \\ J_{l1\_n} = 1.5m_{11|q_2=0} = 1.5\left(L_1^2M_1 + (L_1+L_2)^2M_2\right) \\ k_{1\_n} = 0.5k_1 \\ J_{m2\_n} = 1.3J_2/\gamma_2^2 \\ J_{l2\_n} = 1.5m_2 = 1.5L_2^2M_2 \\ k_{2\_n} = 0.5k_2 \end{cases} \tag{39}$$

where J_{mi_n}, J_{li_n}, k_{i_n} with $i = 1$ to 2 being the nominal values of motor-side inertia, link-side inertia, and joint stiffness of the ith joint, respectively. With the above physical parameter setup, the parameters used to implement the joint torque controller (34) can be given as

$$\begin{cases} \hat{a}_1 = \dfrac{k_{1\_n}}{\gamma_1^2 J_{m1\_n}} + \dfrac{k_{1\_n}}{J_{l1\_n}}, \quad \hat{b}_1 = \dfrac{k_{1\_n}}{\gamma_1^2 J_{m1\_n}} \\ \hat{a}_2 = \dfrac{k_{2\_n}}{\gamma_2^2 J_{m2\_n}} + \dfrac{k_{2\_n}}{J_{l2\_n}}, \quad \hat{b}_2 = \dfrac{k_{2\_n}}{\gamma_2^2 J_{m2\_n}} \end{cases} \tag{40}$$

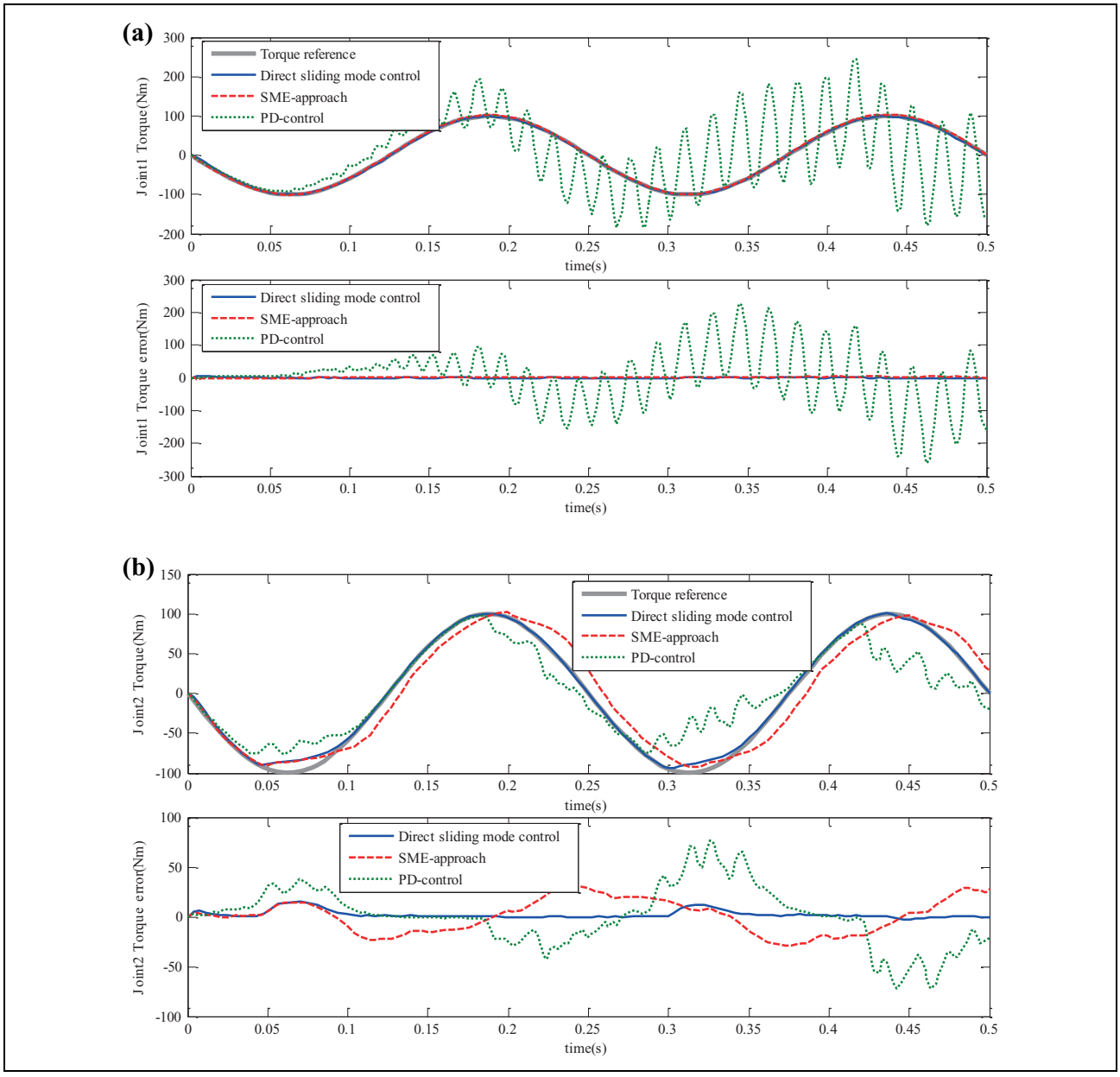

Figure 3. Sinusoidal torque reference (large amplitude): (a) response of joint 1 and (b) joint 2.

Other controller parameters required for this joint torque controller are c_0, c_1, M_s, and the time constant of the low-pass filter. They are selected as

$$\begin{cases} c_{01} = 20{,}000, & c_{11} = 200, & M_{s1} = 2 \times 10^6, & \mu_1 = 1 \times 10^{-3} \\ c_{02} = 20{,}000, & c_{12} = 200, & M_{s2} = 2 \times 10^6, & \mu_2 = 1 \times 10^{-3} \end{cases} \tag{41}$$

where μ_1 and μ_2 are the time constant of the both low-pass filters for both robot joints.

Theoretically, both the direct sliding mode control approach and the SME approach possess the torque tracking control property. The former needs less controller parameters but the second time derivative of the joint torque signal, while the latter needs only the first time derivative of the joint torque signal but much more controller parameters. Thus, there is always some price to pay for a high control performance. As to the differences in the dynamic response of the both joint torque controllers, refer the discussions given below.

Simulation results and discussions

Figures 1 to 6 show the simulation results of the three joint torque controllers applied to the two-link flexible joint robot considering the AC-motor dynamics.

Figures 1 to 3 are for the case of normal flexible joint robots with both joint stiffness $k_1 = k_2$=10,000. From

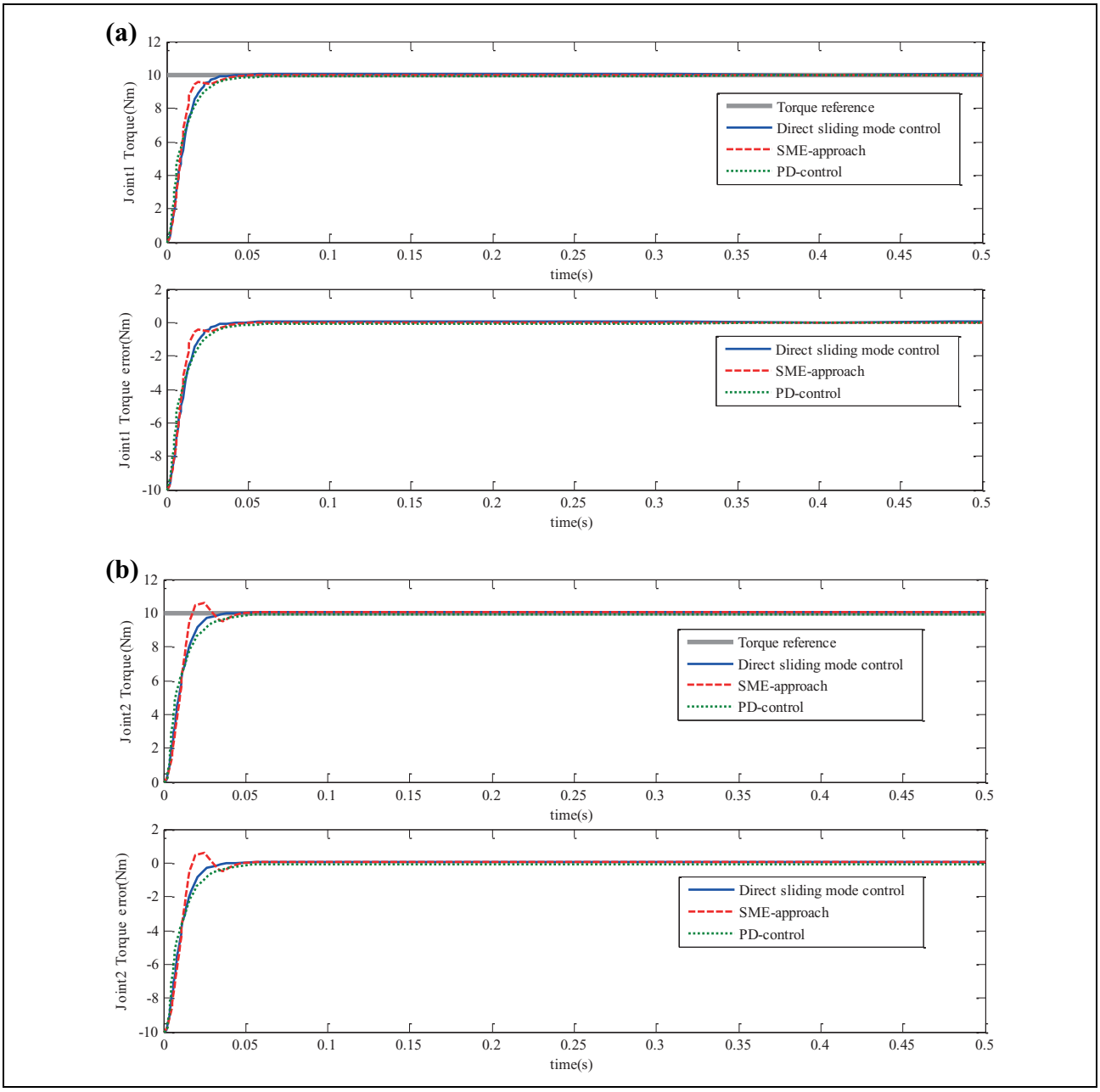

Figure 4. Step response of joint torque control (very large joint compliance): (a) response of joint 1 and (b) joint 2.

Figure 1, we see that the step responses of the direct sliding mode control approach and the SME approach are similar, they converge fast and smoothly to the reference value. The step response of the PD control is a little bit slower and not smooth during the transition phase. The control gains of the PD-controller are set so that the possible fast step response can be reached (just before vibrations occur). For the sinusoidal torque reference of small amplitude (see Figure 2), all three control approaches have similar performance. For the sinusoidal torque reference of large amplitude (see Figure 3), the PD control is unusable, this is because that the PD-control results in a too large and fast changing reference current for the inner current control loop which cannot be followed by the current controller. The SME approach has a time delay in the torque response, see the plot for joint 2 in Figure 3. Among the three control approaches, the direct sliding mode control approach has the best tracking control performance for the case of large sinusoidal torque reference. This result matches the expectation of the author.

Figures 4 to 6 are for the case of the flexible joint robots with very large joint compliance, that is, very low joint stiffness $k_1 = k_2 = 1000$. For the simulations in this category, all other parameters in the controllers and in the plant model remain the same as in the case of normal joint stiffness (i.e. $k_1 = k_1 = 10{,}000$). The step responses of the PD control and the direct sliding mode control, see Figure 4,

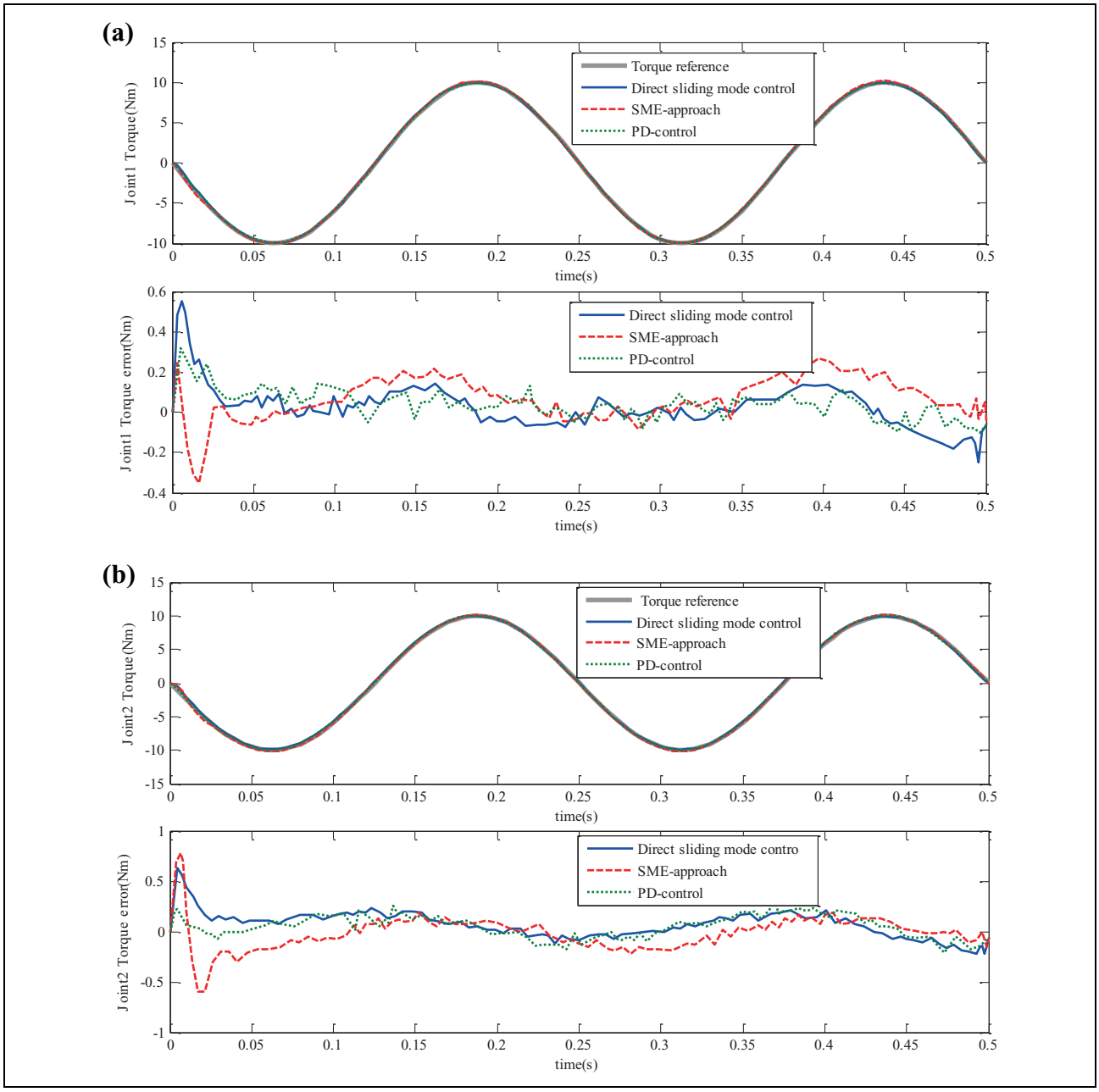

Figure 5. Sinusoidal torque reference (small amplitude, very large joint compliance): (a) response of joint 1 and (b) joint 2.

have no noticeable change with respect to the case of normal joint stiffness (comparing with Figure 1). Now the step response of the SME approach has an overshoot, see the plot for joint 2 in Figure 4. As mentioned before, the SME approach needs the nominal value of some parameters, if these nominal values differ from their true values too much and the controller parameters (including $i_{q\_\max}$ as well as the DC-bus voltage u_0 for the inner current control loop) are not readjusted, the control performance will be changed accordingly. For the sinusoidal torque reference of small amplitude under large joint compliance (see Figure 5), the control performances of all three control approaches have no remarkable change with respect to the case of normal joint stiffness, that is, their control performances are acceptable. For the sinusoidal torque reference of large amplitude under large joint compliance (see Figure 6), the performance of the PD control now becomes much better (because the derivative of the joint torque signal is now much smaller). The tracking control performance of the direct sliding mode control is as good as that of the normal joint stiffness case. The time delay of the SME approach is now enlarged a little bit in some places along the time axis. Again, the direct sliding mode control approach has the best control performance as expected.

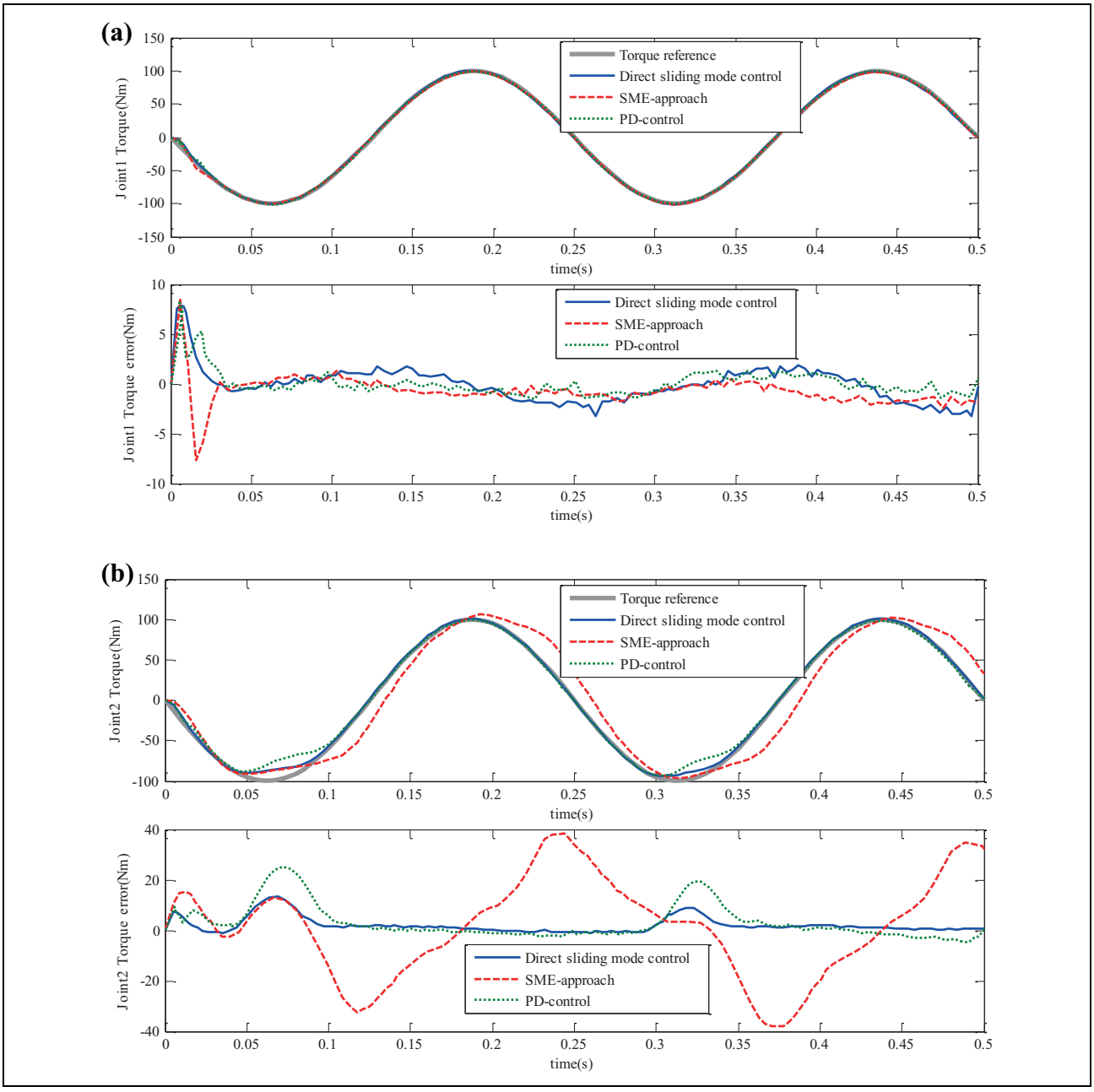

Figure 6. Sinusoidal torque reference (large amplitude, very large joint compliance): (a) response of joint 1 and (b) joint 2.

Conclusions

This article focuses on the joint torque control problems for flexible joint robots. It is emphasized here again that joint torque is a well-selected state variable for the dynamic control issues of this kind of robots, though the control design and implementation is a difficult task. With the decentralized joint torque control schema, the robot dynamics are decoupled (between robot arm and robot joints). Thus, the results for the control of rigid-body arms can be used further. Three joint torque control approaches are proposed: (1) The PD-type controller has some degree of robustness by properly selecting the control gains. (2) The direct sliding mode control approach which fully utilizes the physical properties of electric motors. (3) The SME approach was proposed to compensate the parameter uncertainties and the external disturbances of the joint torque system. These three joint torque controllers are tested and verified by the simulation studies with different reference torque trajectories and under different joint stiffness. As expected, the direct sliding mode control approach showed the best control performance, but for the control implementation, the second time derivative of the joint torque signal is required. The SME approach tries to avoid the second derivative of joint torque signal, but possesses a

more involved control structure and needs more controller parameters; and it generates a time delay when tracking a reference torque signal with large amplitude. The PD-type joint torque controller may become unstable.

Declaration of conflicting interests

The author(s) declared no potential conflicts of interest with respect to the research, authorship, and/or publication of this article.

Funding

The author(s) disclosed receipt of the following financial support for the research, authorship, and/or publication of this article: This project is supported by the National Natural Science Foundation of china (NSFC) [Grant Nos. 61763030, 61263045, 51265034], Jiangxi Province Science and Technology Support Project [Grant No. 20112BB550017], and the Jiangxi Province Natural Science Fund Project [Grant No. 20132BAB201040].

ORCID iD

Gen-Liang Xiong https://orcid.org/0000-0002-1303-6980

References

1. Readman MC. *Flexible joint robots*. Boca Raton: CRC Press, 1994.
2. Kiang CT, Spowage A, and Yoong CK. Review of control and sensor system of flexible manipulator. *J Intell Robot Syst* 2015; 77(1): 187–213.
3. Kostas N, Evangelos G, and Papadopoulos A. On the dynamics and control of flexible joint space manipulators. *Control Eng Pract* 2015; 45: 230–243.
4. Berger RM and ElMaraghy HA. Feedback linearization control of flexible joint robots. *Rob Comput Integr Manuf* 1992; 9(3): 239–246.
5. Dallali H, Lee J, Tsagarakis NG, et al. Experimental study on linear state feedback control of humanoid robots with flexible joints. *IFAC PapersOnLine* 2015; 48(19): 130–135.
6. Akyuz IH, Bingul Z, and Kizir S. Cascade fuzzy logic control of a single-link flexible-joint manipulator. *Turk J Elec Eng Comp Sci* 2012; 20(5): 713–726.
7. Kim J and Croft EA. Full-state tracking control for flexible joint robots with singular perturbation techniques. *IEEE Trans Control Syst Technol* 2017; 99: 1–13.
8. Izadbakhsh A and Masoumi M. FAT-based robust adaptive control of flexible-joint robots: singular perturbation approach. In: *2017 IEEE international conference on industrial technology (ICIT)*, Toronto, Ontario, Canada, 22–25 March 2017, pp. 22–25. IEEE.
9. Ghorbel F and Spong MW. Integral manifolds of singularly perturbed systems with application to rigid-link flexible-joint multibody systems. *Int J Non-Linear Mech* 2000: 35(1): 133–155.
10. Jiang ZH and Shinohara K. Workspace trajectory tracking control of flexible joint robots based on backstepping method. In: *2016 IEEE region 10 conference (TENCON)*, Singapore, Singapore, 22–25 November 2016, IEEE.
11. Reyes-Báez R and van der Schaft AJ. Virtual differential passivity based control for tracking of flexible-joints robots. In: *Workshop on Lagrangian and Hamiltonian methods in nonlinear control*, 1–4 May 2018, pp. 1–8. IFAC.
12. Jin M, Lee J, and Tsagarakis NG. Model-free robust adaptive control of humanoid robots with flexible joints. *IEEE Trans Ind Elect* 2017; 64(2): 1706–1715.
13. Farzanegan B and Banadaki SD. Direct artificial neural network control of single link flexible joint. In: *2016 Fourth international conference on control, instrumentation, and automation (ICCIA)*, Qazvin, Iran, 2016. IEEE.
14. Kim MJ and Chung WK. Disturbance-observer-based PD control of flexible joint robots for asymptotic convergence. *IEEE Trans Robot* 2015; 31(6): 1508–1516.
15. Amjadi F, Khadem S, and Khaloozadeh H. Position and velocity control of a flexible joint robot manipulator via a fuzzy controller based on singular perturbation analysis. In: *Proceedings of 10th annual IEEE conference on fuzzy systems*, Australia, 2001, pp. 348–351.
16. Ott C. *Cartesian impedance control of redundant and flexible-joint robots*. Berlin: Springer, 2008.
17. Yang JM and Kim JH. Sliding mode control for trajectory tracking of nonholonomic wheeled mobile robots. *IEEE Trans Robot Autom* 1999; 15(3): 578–587.
18. Savkin AV and Wang C. A simple biologically-inspired algorithm for collision free navigation of a unicycle-like robot in dynamic environments with moving obstacles. *Robotica* 2013; 31(6): 993–1001.
19. Sarfraz M, Rehman F, and Shah I. Robust stabilizing control of nonholonomic systems with uncertainties via adaptive integral sliding mode an underwater vehicle example. *Int J Adv Robot Syst* 2017; 14(5): 1–11.
20. Ademi S and Jovanović MG. Vector control methods for brushless doubly fed reluctance machines. *IEEE Trans Ind Elect* 2015; 62(1): 96–104.
21. Utkin VI, Guldner J, and Shi J. *Sliding mode control in electromechanical systems*, 2nd ed. Bengaluru: Taylor & Francis, 2009.

Appendix 1

1. The block diagrams of three joint torque control approaches:

   (1) joint torque control by PD controller,
   (2) joint torque control by direct sliding mode control, and
   (3) joint torque control by SME.

2. The stability of the controller (34) along with observer described in the "Joint torque control by SME" section is proved.

The proof of stability process is as follows:

Design control τ_f as

$$\tau_f = \hat{b}^{-1}(\hat{a}\tau + \ddot{\tau}_d - c_1\dot{e}_\tau - c_0 e_\tau) \tag{1A}$$

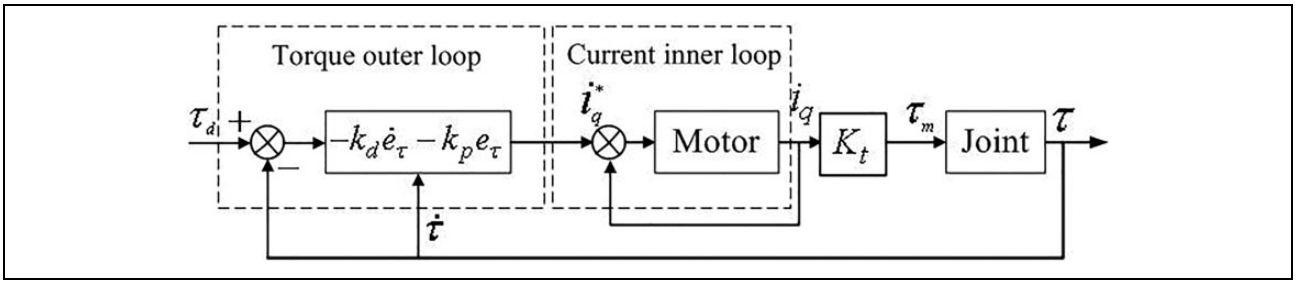

Figure A1. The block diagram of joint torque control by PD controller.

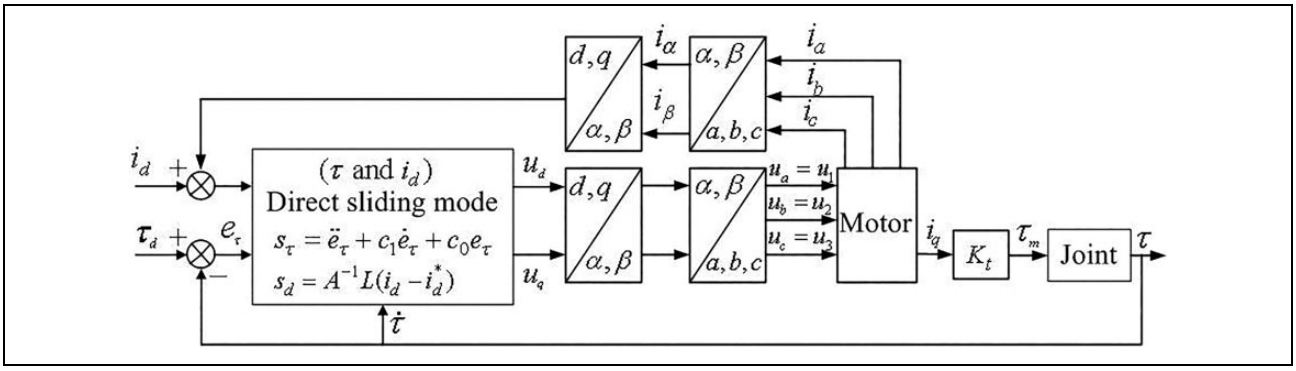

Figure A2. The block diagram of joint torque control by direct sliding mode controller.

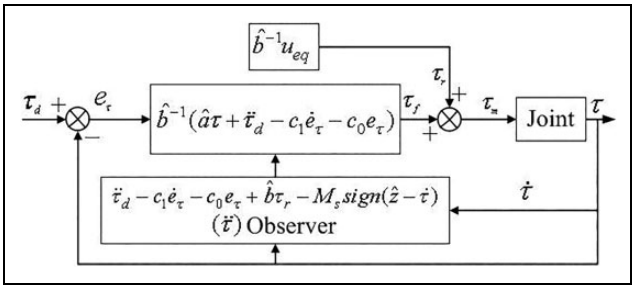

Figure A3. The block diagram of joint torque control by sliding mode estimator.

where $\hat{a}$ and $\hat{b}$ are estimates (or called nominal values) of a and b, respectively, and $e_\tau = \tau_d - \tau$ is the torque control error. The first term $\hat{b}^{-1}\hat{a}\tau$ in equation (1A) seeks to compensate the term $b^{-1}a\tau$ in model (33) (in this article) as a type of feedback linearization. The second term in (1A), $\hat{b}^{-1}\ddot{\tau}_d$, is a feed-forward term of acceleration of the desired torque. Finally, the last two terms in (1A), $\hat{b}^{-1}(c_1\dot{e}_\tau + c_0 e_\tau)$, are a linear pole placement controller. Substitution of equation (1A) into equation (33) yields error dynamics for $e_\tau = \tau_d - \tau$, $\dot{e}_\tau = \dot{\tau}_d - \dot{\tau}$, and $\ddot{e}_\tau = \ddot{\tau}_d - \ddot{\tau}$ as

$$\ddot{e}_\tau + c_1\dot{e}_\tau + c_0 e_\tau = \tau_p - \hat{b}\tau_r \tag{1B}$$

The left-hand side of equation (1B) is linear with poles determined by $c_0, c_1 > 0$, but is subjected to the perturbation term

$$\tau_p = \left(\frac{\hat{b}}{b} - 1\right)\ddot{\tau} + \left(\frac{\hat{b}}{b}a - \hat{a}\right)\tau + \frac{\hat{b}}{b}d \tag{1C}$$

which may be simplified by substitution of $\ddot{\tau} = b\tau_m - a\tau - d$ from equation (33) to

$$\tau_p = (a - \hat{a})\tau + (\hat{b} - b)\tau_m + d \tag{1D}$$

In order to improve the control performance, the disturbance (1D) should be compensated for by the additional disturbance rejection term τ_r in $\tau_m = \tau_f + \tau_r$. Because τ_p is immeasurable, an estimate can be obtained using a sliding mode observer of the form

$$\dot{\hat{z}} = \ddot{\tau}_d + c_1\dot{e}_\tau + c_0 e_\tau + \hat{b}\tau_r - u \tag{1E}$$

with $\hat{z}$ being an estimate for $\dot{\tau}$. Basically, observer (1E) is a copy of equation (1B) with $\ddot{\tau} = \dot{\hat{z}}$ and observer feedback term u as a replacement for τ_p being defined as

$$u = (\bar{a}^+|\tau| + \bar{b}^+|\tau_m| + \bar{d}^+)\text{sign}\bar{z} \tag{1F}$$

Here, $\bar{a}^+$, $\bar{b}^+$, and $\bar{d}^+$ denote upper bounds for $\bar{a}$, $\bar{b}$, and $\bar{d}$, respectively, obtained from the bounds on the system parameters and given as follows

$$\begin{cases} \bar{a} = \max\left\{ \left(\dfrac{k^+}{\gamma^2 J_m^-} + \dfrac{k^+}{J_l^-} \right) - \hat{a}, \hat{a} - \left(\dfrac{k^-}{\gamma^2 J_m^+} + \dfrac{k^-}{J_l^+} \right) \right\} \\ \bar{b} = \max\left\{ \dfrac{k^+}{\gamma J^-} - \hat{b}, \hat{b} - \dfrac{k^-}{\gamma J^+} \right\} \\ \bar{d} = \left(\dfrac{k^+}{\gamma J^-} \right) d_m + \dfrac{k^-}{J^+} d_l \end{cases} \tag{1G}$$

where $J_l^- \leq J_l \leq J_l^+$ is the link inertia, $J_m^- \leq J_m \leq J_m^+$ is the motor/gear inertia, and $k^- \leq k \leq k^+$ denotes the joint stiffness.

The control discontinuity, denoted by the signum function sign() in equation (1F), is introduced along the observation error $\bar{z} = \hat{z} - \dot{\tau}$. Note that for the implementation of observer (1E), an initial value of τ_r is required. Because the control gain of u should be high enough to enforce the sliding mode, the response of the observer (1E) is insensitive to this initial value $\tau_r(0)$, implying that $\tau_r(0) = 0$ can be used for the first calculation loop. Another remark needs to be made is about the term τ_m in equation (1F). As will be shown later, the real control input τ_m is a quasi-continuous term, thus the control gain of u can be found to enforce the sliding mode.

Stability of the observer system is ensured via *Lyapunov* function candidate $V = \frac{1}{2}\bar{z}^2$; differentiation along the system trajectories (1E) with control (1F) yields

$$\begin{aligned} \dot{V} &= \left(\ddot{\tau}_d + c_1 \dot{e}_\tau + c_0 e_\tau + \hat{b}\tau_r - (\bar{a}^+|\tau| + \bar{b}^+|\tau_m| + \bar{d}^+)\mathrm{sign}\bar{z} - \ddot{\tau} \right)\bar{z} \\ &= \tau_p \bar{z} - \tau_p^+ |\bar{z}| \end{aligned} \tag{1H}$$

where $\tau_p^+ = \bar{a}^+|\tau| + \bar{b}^+|\tau_m| + \bar{d}^+ > \max(\tau_p)$ ensures the existence of sliding mode via

$$\dot{V} < 0 \tag{1I}$$

Because observer (1E) is calculated in the control computer, the initial condition can be set as

$$\hat{z}(0) = \dot{\tau}(0) \tag{1J}$$

such that $\bar{z}(t) \equiv 0$ for all $t \geq 0$, that is, sliding mode is initiated immediately at $t = 0$.

In order to estimate the disturbance torque τ_p to be compensated via disturbance rejection term τ_r in $\tau_m = \tau_f + \tau_r$, the equivalent control method, see Utkin,[1] is exploited here once again. In sliding mode, we have $\dot{\bar{z}} = \dot{\hat{z}} - \ddot{\tau} = 0$, that is

$$\dot{\bar{z}} = \dddot{e}_\tau + c_1 \ddot{e}_\tau + c_0 \dot{e}_\tau + \hat{b}\dot{\tau}_r - \dot{u}_{\mathrm{eq}} = 0 \tag{1K}$$

The control signal u in equation (1F) contains two components: a high-frequency switching component resulting from the discontinuous signum term and a low-frequency component, that is, the equivalent control u_{eq}. As discussed in detail in Utkin,[1] the equivalent control is equal to the average value of u, obtained by a low-pass filter. With this in mind, $u_{\mathrm{eq}} = u_{av} = \tau_p = \text{low-pass}\left(M_s \mathrm{sign}(\hat{z} - \dot{\tau})\right)$ follows from comparing equations (1B) and (1K). Consequently, selecting

$$\tau_r = \hat{b}^{-1} u_{\mathrm{eq}} = \hat{b}^{-1} u_{av} \tag{1L}$$

leads to a closed-loop error dynamics

$$\dddot{e}_\tau + c_1 \ddot{e}_\tau + c_0 \dot{e}_\tau = 0 \tag{1M}$$

where u_{av} can be obtained by a low-pass filter with the discontinuous control u given in (1F) as the filter input.

Hence, sliding mode estimator τ_r successfully rejects both the uncertainties in parameters a and b, and the additive disturbance d in equation (33) and allows controller (1A) to perform exact pole placement. It should be noted that the time constant or the bandwidth of the low-pass filter has to be carefully chosen: to be faster than the perturbation dynamics given by equation (1C) for a successful rejection of τ_p, but at the same time slow enough to avoid exciting unmodeled dynamics (e.g. the neglected actuator dynamics). In practical applications, since the spectrum of the perturbation dynamics does not come into the spectrum of the high-frequency switching (after sliding mode occurs), a trade-off can normally be found for the selection of the filter time constant. It should be pointed out that for this SME design, only the first time derivative of the joint torque signal is required, whereas the approach given by Elmali and Olgac[2] would need the second time derivative of the joint torque. Moreover, there is no need to assume that the time-derivative of the system perturbation is equal to zero.

1. Utkin VI. *Sliding modes in control and optimization*. London, UK: Springer-Verlag, 1992.
2. Elmali H and Olgac N. Theory and implementation of sliding mode control with perturbation estimation. In: Proceedings of the IEEE ICRA'92, Nice, France, 12–14 May 1992, pp. 2114–2119. IEEE.